Respiratory Medicine 112 (2016) 10–17

Contents lists available at ScienceDirect

Respiratory Medicine

journal homepage: www.elsevier.com/locate/rmed

Review article

Thoracic lymphadenopathy in benign diseases: A state of the art review

Carlos Schüler Nin [a, 1], Vinícius Valério Silveira de Souza [a, 2], Ricardo Holderbaum do Amaral [a, 3], Roberto Schuhmacher Neto [a, 4], Giordano Rafael Tronco Alves [b, 5], Edson Marchiori [b, 6], Klaus Loureiro Irion [c, 7], Fernanda Balbinot [a, *, 8], Gustavo de Souza Portes Meirelles [d, 9], Pablo Santana [e, 10], Antônio Carlos Portugal Gomes [e, 11], Bruno Hochhegger [a, 12]

[a] Federal University of Health Sciences of Porto Alegre, Porto Alegre, Brazil
[b] Federal University of Rio de Janeiro, Rio de Janeiro, Brazil
[c] Liverpool Heart and Chest Hospital, Liverpool, United Kingdom
[d] Fleury Medicina Diagnóstica, São Paulo-SP, Brazil
[e] Hospital São Joaquim Beneficência Portuguesa, São Paulo-SP, Brazil

ARTICLE INFO

Article history:
Received 15 June 2015
Received in revised form
14 November 2015
Accepted 28 January 2016
Available online 1 February 2016

Keywords:
Lymphadenopathy

ABSTRACT

Lymphadenopathy is a common radiological finding in many thoracic diseases and may be caused by a variety of infectious, inflammatory, and neoplastic conditions. This review aims to describe the patterns of mediastinal and hilar lymphadenopathy found in benign diseases in immunocompetent patients. Computed tomography is the method of choice for the evaluation of lymphadenopathy, as it is able to demonstrate increased size of individual nodes, abnormalities of the interface between the mediastinum and lung, invasion of surrounding fat, coalescence of adjacent nodes, obliteration of the mediastinal fat, and hypo- and hyperdensity in lymph nodes. Intravenous contrast enhancement may be needed to help distinguish nodes from vessels. The most frequent infections resulting in this finding are tuberculosis and

* Corresponding author. Rua Coronel Vicente, 451. Centro, CEP 90030041, Porto Alegre, Rio Grande do Sul, Brazil.
E-mail addresses: carlos.s.nin@gmail.com (C.S. Nin), viniciusvss@gmail.com (V.V.S. de Souza), rh.doamaral@gmail.com (R.H. do Amaral), npcbeto@hotmail.com (R.S. Neto), grtalves@gmail.com (G.R. Tronco Alves), edsonmarchiori@gmail.com (E. Marchiori), klaus.irion@lhch.nhs.uk (K.L. Irion), balbinotf@gmail.com (F. Balbinot), brunohochhegger@gmail.com (B. Hochhegger).
[1] Tel.: +55 5132148504. Institutional address: Irmandade Santa Casa de Misericórdia de Porto Alegre, LABIMED - Laboratório de Pesquisas em Imagens Médicas. Rua Prof. Annes Dias, 28; Centro; Porto Alegre, RS; Brazil; ZIP code: 9002009.
[2] Tel.: +55 5132148504. Institutional address: Irmandade Santa Casa de Misericórdia de Porto Alegre, LABIMED - Laboratório de Pesquisas em Imagens Médicas. Rua Prof. Annes Dias, 28; Centro; Porto Alegre, RS; Brazil; ZIP code: 90020090.
[3] Tel.: +55 5132148504. Institutional address: Irmandade Santa Casa de Misericórdia de Porto Alegre, LABIMED - Laboratório de Pesquisas em Imagens Médicas. Rua Prof. Annes Dias, 28; Centro; Porto Alegre, RS; Brazil; ZIP code: 90020090.
[4] Tel.: +55 5132148504. Institutional address: Irmandade Santa Casa de Misericórdia de Porto Alegre, LABIMED - Laboratório de Pesquisas em Imagens Médicas. Rua Prof. Annes Dias, 28; Centro; Porto Alegre, RS; Brazil; ZIP code: 90020090.
[5] Tel.: +55 21 26202828. Institutional address: Federal University of Rio de Janeiro. Rua Thomaz Cameron, 43; Valparaíso, Petrópolis, Rio de Janeiro; Brazil; ZIP code: 25685120.
[6] Tel.: +55 21 26202828. Institutional address: Federal University of Rio de Janeiro. Rua Thomaz Cameron, 438; Valparaíso, Petrópolis, Rio de Janeiro; Brazil; ZIP code: 25685120.
[7] Tel.: +44 15 1617679073. Institutional address: Liverpool Heart and Chest Hospital, NHS Foundation Trust, Department of Radiology. Thomas Drive Broadgreen, Liverpool; United Kingdom; ZIP code: L143PE.
[8] Tel.: +55(51)30247347. Institutional address: Irmandade Santa Casa de Misericórdia de Porto Alegre, LABIMED - Laboratório de Pesquisas em Imagens Médicas. Rua Prof. Annes Dias, 28; Centro; Porto Alegre, RS; Brazil; ZIP code: 90020090.
[9] Tel.: +551159087901. Institutional address: Universidade Federal de São Paulo, Departamento de Diagnóstico Por Imagem. Rua Napoleão de Barros, 800; Vila Clementino, São Paulo - SP, Brazil; Zip code: 04024002.
[10] Tel.: +551135051000. Institutional address: Hopsital São Joaquim beneficência Portugues. Departamento de Radiologia e Diagnóstico por Imagem. Rua Maestro Cardim, 769; Liberdade, São Paulo - SP, Brazil. Zip Code: 01323001.
[11] Tel.: +551135051000. Institutional address: Hopsital São Joaquim beneficência Portugues. Departamento de Radiologia e Diagnóstico por Imagem. Rua Maestro Cardim, 769; Liberdade, São Paulo - SP, Brazil. Zip Code: 01323001.
[12] Tel.: +55 5132148504. Institutional address: Irmandade Santa Casa de Misericórdia de Porto Alegre, LABIMED - Laboratório de Pesquisas em Imagens Médicas. Rua Prof. Annes Dias, 28; Centro; Porto Alegre, RS; Brazil; ZIP code: 90020090.

http://dx.doi.org/10.1016/j.rmed.2016.01.021

Thoracic disease
Benign disease
Computed tomography

fungal disease (particularly histoplasmosis and coccidioidomycosis). Sarcoidosis is a relatively frequent cause of lymphadenopathy in young adults, and can be distinguished from other diseases – especially when enlarged lymph nodes are found to be multiple and symmetrical. Other conditions discussed in this review are silicosis, drug reactions, amyloidosis, heart failure, Castleman's disease, viral infections, and chronic obstructive pulmonary disease.

Contents

1. Introduction

Lymphadenopathy refers to the abnormality of lymph node size, density, and/or number [1]. Computed tomography (CT) is the method of choice for the evaluation of these features. CT findings in thoracic lymphadenopathy include loss of normal ovoid shape, increased size of individual nodes, focal contour abnormalities, hypo- or hyperdensity in lymph nodes, invasion of surrounding mediastinal fat, coalescence of adjacent and enlarged nodes, and diffuse soft-tissue attenuation through the mediastinum, obliterating the mediastinal fat [2,3].

Frequent causes of lymphadenopathy are inflammatory and neoplastic conditions, as well as several infections. Thus, numerous features should be considered when assessing nodal disease to distinguish benign from malignant nodes [1]. A normal node tends to have a uniform appearance. The presence of fat often (but not invariably) indicates benignity. Malignant nodes, on the other hand, exhibit irregular borders and tend to be more round than elongated [4]. Heterogeneous enhancement of an enlarged node is also likely to represent malignancy, although this feature may be seen in benign diseases, such as tuberculosis (TB) [5,6].

Regarding benign etiologies, the most common infections that result in thoracic lymphadenopathy are TB and fungal disease (primarily histoplasmosis and coccidioidomycosis). Sarcoidosis is a particularly frequent cause of this condition in young adults. Other causes include silicosis, drug reactions, amyloidosis, heart failure, Castleman's disease, and chronic obstructive pulmonary disease (COPD) [7]. The aim of this review is to describe the patterns of mediastinal and hilar lymphadenopathy found in benign diseases in immunocompetent patients.

1.1. Lymph node measurement and criteria for lymph node enlargement

For the diagnosis of pathologically enlarged nodes, information about normal node size is required. Commonly used metrics for lymph node measurement include the maximum and minimum axial diameters, and the ratio of these two values [8]. The shortest axial diameter appears to be a more useful parameter than the greatest axial diameter, although a different threshold should be used for each nodal station [5,8,9].

The generally accepted size criterion for mediastinal lymph node enlargement (>10 mm along the short axis) has been applied to all patients when staging lymphoma or bronchogenic carcinoma [10]. Other authors use the following standard maximum normal short-axial diameters for nodal regions: region 7, 12 mm; regions 4 and 10R, 10 mm; and other regions, 8 mm. Maximum greatest axial diameters show wider variation, ranging from 10 to 25 mm [9].

Lymph node location and age must also be taken into account when evaluating lymph nodes in the pediatric chest. At least one enlarged lymph node was found in 96% of children, with subcarinal (69%), lower paratracheal (64%), and hilar (60%) nodes being most common. Up to 10 years of age, most lymph nodes are $\leq$7 mm in diameter. In older children, lymph nodes with short-axis diameters of up to 10 mm have been found [11].

1.2. Tuberculosis

TB is an airborne infectious disease caused by *Mycobacterium tuberculosis*. It can be divided into primary and postprimary TB, based on the absence or presence of prior infection and acquired specific immunity, although the radiological appearances of these manifestations overlap considerably [12].

Primary TB is most commonly seen in children. The initial focus of infection —the Ghon focus —tends to be in the middle and lower

lobes of the lung due to their ventilatory pattern and volume, although any lobe can be affected [12]. During the early stage of infection, mycobacteria are commonly spread to regional lymph nodes and via the bloodstream to other regions of the body. The term utilized to refer the Ghon focus plus affected lymph nodes is the "Ghon complex". Although this complex may enlarge as the disease progresses, it commonly undergoes a healing process, resulting in a visible parenchymal scar (which may be calcified) and enlarged or calcified nodes in the hilus or mediastinum [13,14].

Lymphadenopathy is the main feature of primary TB. It is observed in 40% of adult cases and 90–95% of pediatric cases [14]. Unilateral compromise is usually present, and hilar lymph nodes are most often affected. On CT, the most suggestive aspect of primary TB consists of enlarged lymph nodes –generally >2 cm in diameter– with hypodense centers secondary to caseous necrosis, as well as a peripheral denser area that increases after the administration of contrast, representing a rim of granulomatous inflammatory tissue (Fig. 1) [6].

Postprimary TB is a progressive condition that is rarely associated with lymphadenopathy. It usually presents as parenchymal, airway, and pleural involvement. Hilar and mediastinal lymphadenopathy occur in only approximately 5% of immunocompetent patients [12].

1.3. Fungal infections

Fungal infections, most notably histoplasmosis and pulmonary coccidioidomycosis, can cause lymph node enlargement. The former is a systemic infection that results from the inhalation of airborne spores of *Histoplasma capsulatum*. In the acute form of this disease, lymphadenopathy is a common finding (Fig. 2) and calcifications may be seen (Fig. 3) [15]. In the chronic form, however, this finding is unusual, and the radiological manifestations are very similar to those of postprimary pulmonary TB.

Direct infection of lymph nodes by *H. capsulatum* may lead to the development of mediastinal granuloma –a mediastinal mass made up of enlarged, caseous lymph nodes, sometimes partly liquefied and surrounded by a thin fibrous capsule. Some authors believe that this granuloma can lead to fibrosing mediastinitis, presenting as a proliferation of fibrous tissue within the mediastinum and, in some instances, within the lumina of mediastinal vessels and airways [16,17]. Thus, these authors argue that mediastinal granulomas should be resected when discovered, even in the absence of presenting symptoms.

Coccidioidomycosis is a systemic mycosis caused by inhalation of arthrospores of *Coccidioides* species. It can be divided into acute, disseminated, and chronic forms, each with a spectrum of imaging findings [18]. CT shows hilar or mediastinal lymphadenopathy associated with parenchymal abnormalities in 40% of patients with the acute form of this disease [19]. Mediastinal lymphadenopathy may persist after parenchymal abnormalities resolve; in such cases, it has been proposed as a risk factor for disseminated infection [20,21]. Nevertheless, consensus on this issue is lacking [22]. In disseminated coccidioidomycosis, hilar and mediastinal lymphadenopathy is usually present, in association with miliary nodules and confluent parenchymal opacities. Imaging manifestations of the chronic form of the disease include residual nodules, chronic cavities, pleural effusion, and persistent pneumonia with or without lymphadenopathy [18].

1.4. Sarcoidosis

Sarcoidosis is a systemic granulomatous disease that affects primarily the lung and lymphatic system. Five radiological stages of intrathoracic changes have been defined: stage 0, no visible intrathoracic finding; stage 1, lymphadenopathy only; stage 2, lymphadenopathy with parenchymal infiltration; stage 3, parenchymal disease only; and stage 4, pulmonary fibrosis [23].

Lymphadenopathy is seen in stages 1 and 2. The most common pattern is bilateral hilar and right paratracheal lymphadenopathy, also known as Garland's triad. The left paratracheal nodes and the aortopulmonary window nodes are also commonly enlarged [24]. In general, when multiple lymph node groups in the hila and mediastinum are symmetrically enlarged in a young patient, sarcoidosis is the most likely diagnosis (Fig. 4). Amorphous, punctate, or eggshell-like calcifications may also be seen and are suggestive of a chronic condition, occurring in 3% of patients after 5 years and in 20% after 10 years [25].

Symmetry of hilar lymphadenopathy is an important feature differentiating sarcoidosis from alternative diagnoses, such as lymphoma, fungal disease, and TB [24]. Unilateral hilar adenopathy occurs in only 3–5% of sarcoidosis cases and is the most common atypical manifestation of the disease in patients aged >50 years [26]. Mediastinal lymphadenopathy without hilar lymphadenopathy is an unusual finding [24]. The involvement of the anterior or posterior mediastinal lymph nodes is also infrequent and should call into question the diagnosis of sarcoidosis [27].

1.5. Silicosis

Silicosis is caused by the inhalation of free silica particles during occupational exposure –such as in mining, drilling, and

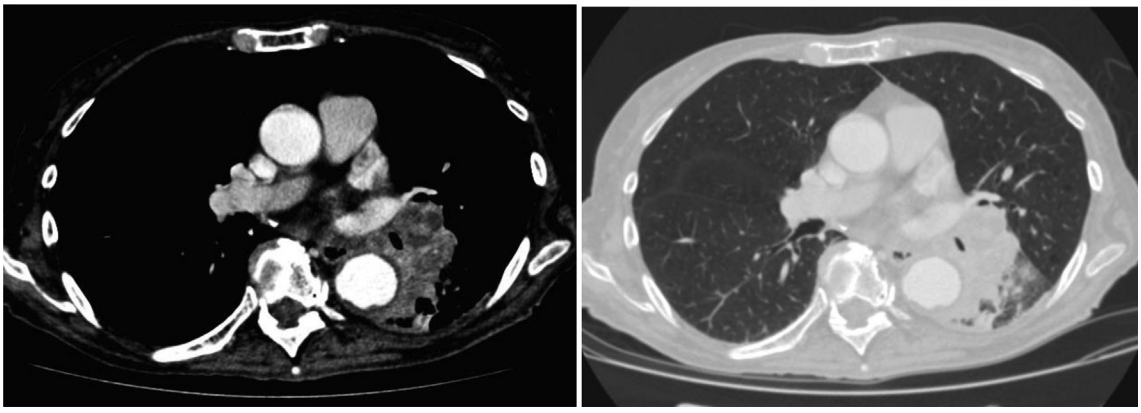

Fig. 1. CT images from a 53-year-old man presenting with cough and fever, demonstrating left hilar hypodense lymphadenomegaly and leading to the diagnosis of lymph node tuberculosis.

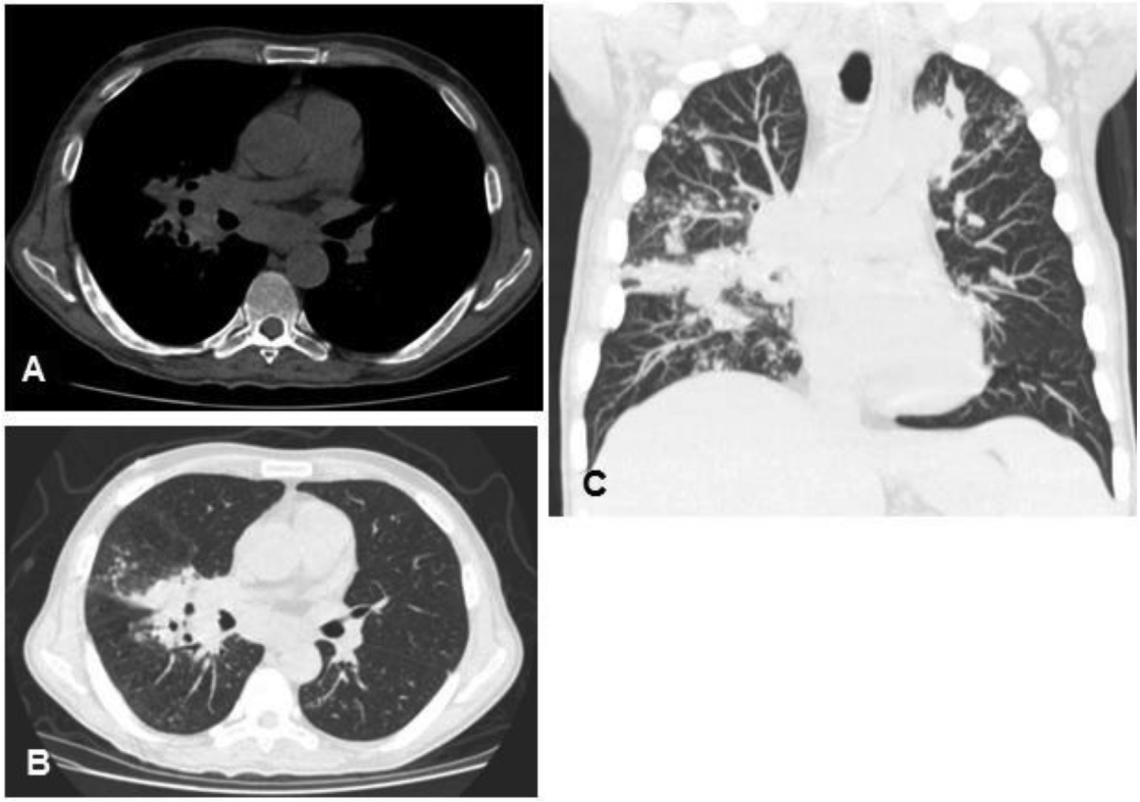

Fig. 2. CT images from a 36-year-old man presenting with cough, fever, and weight loss. (A,B) The images reveal subcarinal lymphadenomegaly and cavitated lesions on the upper right lobe. (C) CT with coronal reconstruction demonstrated tree-in-bud centrolobular nodular disease in the right lung and left upper lobe. A biopsy of this node revealed tuberculosis.

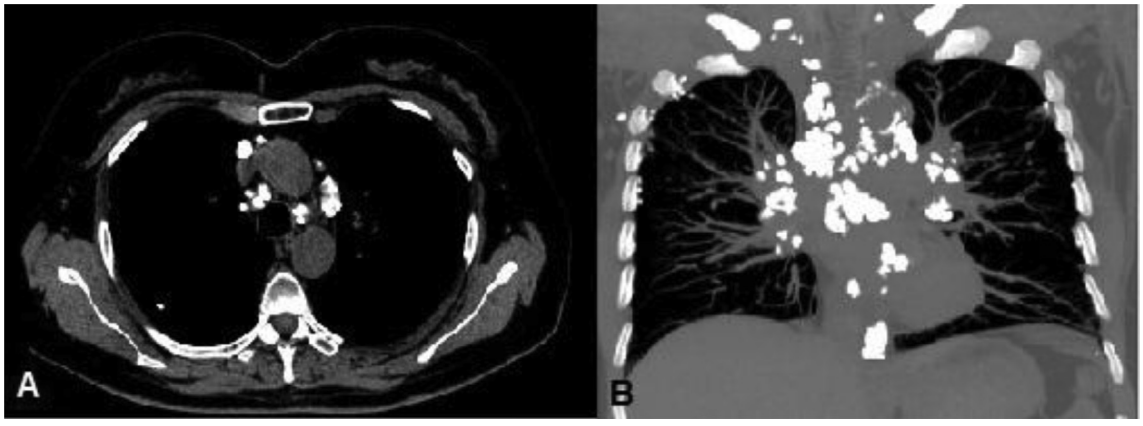

Fig. 3. CT images from a 55-year-old woman presenting with chronic cough, fever, and weight loss. Axial reconstruction of images obtained in the aortopulmonary window shows calcified lymph nodes with diameters >1.2 cm(A), best demonstrated on maximum-intensity projection(B). A lymph node biopsy revealed histoplasmosis.

sandblasting —which leads to a fibrous tissue reaction in the lungs [28]. The classical features of patients with silicosis are diffuse interstitial shadowing with bilateral enlargement of hilar lymph nodes, which may or may not be calcified [29]. Antao et al. [30] also found that 74% of silicotic patients had enlarged mediastinal lymph nodes and 66% of exposed workers had evidence of lymph node calcification. Eggshell calcification is the most common pattern described in silicosis (Fig. 5) [28,31,32], although some authors have reported that the puncate pattern is most prevalent [30,33].

Hilar and mediastinal lymphadenopathy have been suggested to precede lung parenchymal silicosis [28,34,35]. Cox-Grasner et al. [36] found that 90% of subjects with parenchymal silicosis had accompanying fibrotic lymph nodes. These findings support the hypothesis that lymph node fibrosis impairs the elimination of silica dust from the lungs, increasing the lung dust burden and reflecting an additional risk for parenchymal silicosis.

1.6. Amyloidosis

Amyloidosis is characterized by the accumulation of inappropriately folded protein deposits. It may be localized, but it is much more commonly diffuse, affecting organ function by replacing the

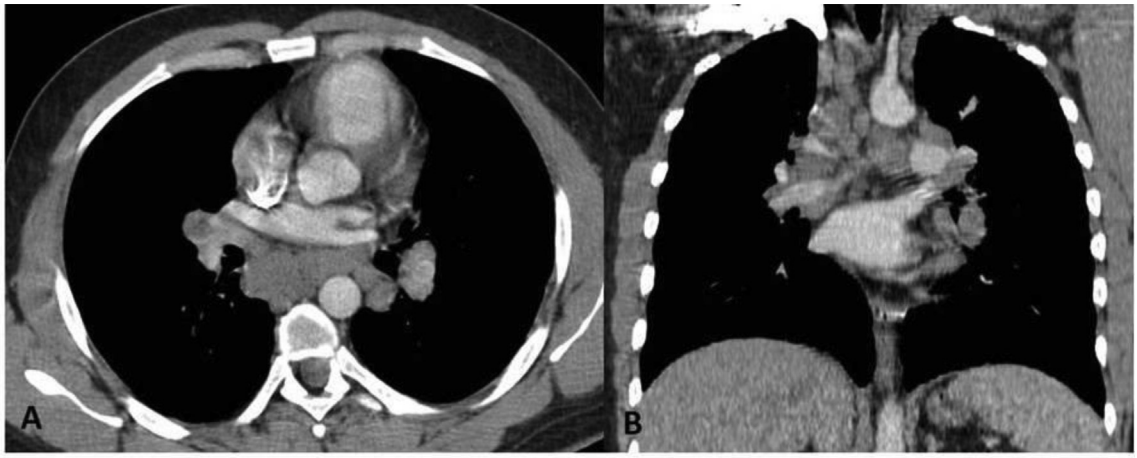

Fig. 4. CT images from a 42-year-old woman presenting with chronic dyspnea. Axial (A) and coronal (B) reconstructions reveal pathologically enlarged mediastinal and hilar lymph nodes. A lymph node biopsy revealed sarcoidosis.

normal cell structure. Based on the structure of the fibrillar protein —one of the deposit's components—amyloidosis is classified into several types, most commonly primary and secondary [37].

Hilar and mediastinal lymph node enlargement is not described in secondary amyloidosis, and is uncommon in localized amyloidosis. However, it is quite common in primary amyloidosis. Thoracic lymphadenopathy, alone or with interstitial disease, is the most common CT finding in primary amyloidosis. Mediastinal and hilar lymph nodes may be involved, bilaterally and often massively, resulting in a pattern that may resemble sarcoidosis. Calcification is usually described as coarse or nonspecific, and eggshell calcification may be seen. Associations with nephrotic syndrome, congestive heart failure, and neuropathy can help identify the disease [7].

1.7. Berylliosis

Berylliosis is a lung disease caused by the inhalation of beryllium (Be) compounds. It can lead to acute chemical pneumonitis — due to intense exposure to Be within a short time — or chronic interstitial lung disease, after prolonged exposure to lower Be concentrations. The chronic form is more common and presents as intraalveolar accumulation of lymphocytes and macrophages, alveolitis, and noncaseating granulomas [38].

CT appearances of chronic Be disease are similar to those of sarcoidosis, although mediastinal and hilar lymphadenopathy are less common, occurring in about 25% of patients. Be disease should be included in the differential diagnosis for all patients with imaging appearances suggestive of sarcoidosis [39].

1.8. Castleman's disease

Castleman's disease is an uncommon, mainly benign, lymphoproliferative disorder of unknown etiology. The overall prevalence of the disease is estimated to be less than 1/100,000 [40]. Castleman's disease may be localized or multifocal. The former presents few or no symptoms, so its diagnosis is made typically through incidental radiological findings. On chest radiographs, it may appear as an incidental, rounded, solitary mediastinal or hilar mass with a differential diagnosis that includes thymoma, lymphoma, neurogenic tumor, and bronchial adenoma [41]. On CT, it usually manifests as a homogeneous, noninvasive, large, solitary mass with soft-tissue attenuation (Fig. 6), most commonly in the mediastinum

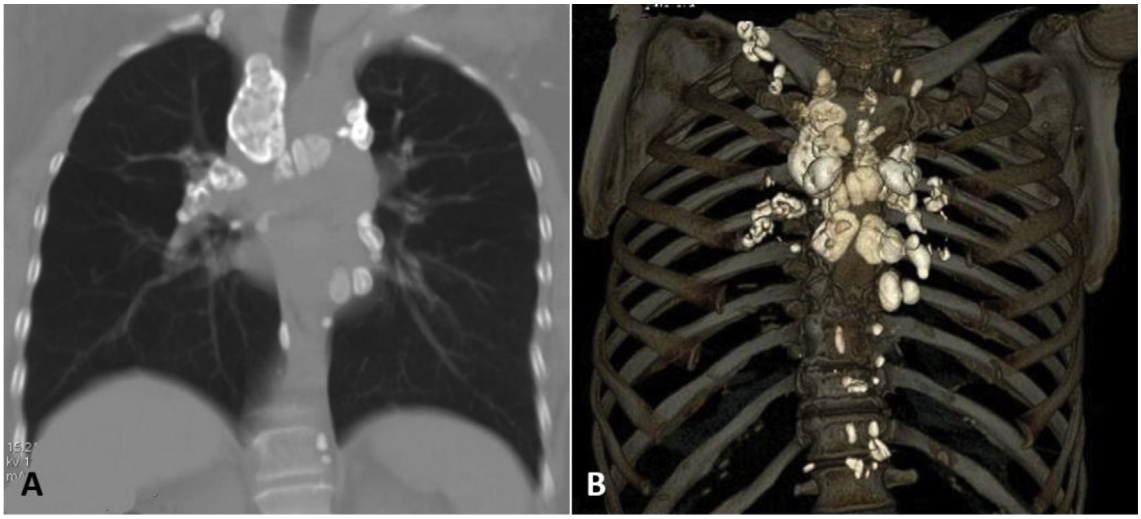

Fig. 5. Images from a 62-year-old male coal worker presenting with chronic cough and dyspnea. Note the extensive eggshell-like lymph node appearance at all stations on the coronal CT reconstruction (A) and 3D volume rendering (B). An open lung biopsy confirmed the diagnosis of silicosis.

Fig. 6. Images from a 42-year-old man with acute viral infection whose x-ray showed widening of the mediastinum. (A, B) CT confirmed lymph node enlargement, especially in the subcarinal region. (C) Positron emission tomography shows increased ^{18}F-FDG uptake. A biopsy of this node revealed Castleman's disease.

or hila [42].

Other patterns that may be seen in the localized form of this disease are a dominant mass with involvement of contiguous structures and, less frequently, matted lymphadenopathy confined to a single mediastinal compartment [41]. Hypervascularity of the lesion may lead to homogeneously intense enhancement following administration of contrast. Intralesional calcifications are uncommon (occurring in 5–10% of cases); when present, they are typically coarse and central [41,42].

Multifocal Castleman's disease presents with inflammatory symptoms including fever, night sweats, weight loss, and anemia. Currently, it is most commonly diagnosed in individuals infected with HIV-1, although it certainly can develop in immunocompetent individuals [43–45]. Multifocal Castleman's disease manifests itself with generalized lymphadenopathy [46]. In patients with multifocal disease, thoracic imaging may show bilateral hilar and mediastinal enlargement of lymph nodes (1–3-cm diameters), as well as diffuse reticulonodular pulmonary infiltrations [41,47]. However, radiological findings are not sufficiently reliable to establish a diagnosis of Castleman's disease, which requires histological confirmation [46].

1.9. Viral infections

Several viruses, including Epstein–Barr virus (EBV), varicella-zoster virus, hantaviruses, influenza viruses, and dengue virus, can cause lower respiratory tract infection in immunocompetent adults. Radiological manifestations of viral infections include small ill-defined nodules, ground-glass opacities, and areas of consolidation. Thoracic lymphadenopathy may also be found, although it is not common [48].

Among these viruses, lymphadenopathy is among the main features of EBV. Infectious mononucleosis –caused by primary infection by this virus– manifests with the typical triad of fever, pharyngitis, and lymphadenopathy, often accompanied by splenomegaly [49]. Despite its importance, however, reports of hilar lymphadenopathy associated with EBV have been confined largely to the radiological literature [50].

Varicella-zoster virus infection manifests primarily as chickenpox or herpes zoster, and is more commonly seen in children [49]. The disease can evolve to pneumonia, more commonly in pregnant and immunosuppressed patients [51,52]. Imaging of the chest in varicella pneumonia usually shows diffuse nodules, sometimes coalescent, with a surrounding halo of continuous or patchy ground-glass opacity. Although uncommon, lymphadenopathy may be seen [53]. Maher et al. [54] found mediastinal lymphadenopathy in a patient with this type of pneumonia after lung transplantation. Hilar lymphadenopathy –which subsided as the pulmonary infection resolved –has also been reported [55].

The genus *Hantavirus* chronically infects rodents without apparent disease; when spread to humans, it can lead to hemorrhagic fever with renal syndrome (HFRS) and hantavirus pulmonary syndrome (HPS), both accompanied by myocardial depression and hypotension or shock [56]. Reports of thoracic lymphadenopathy in hantavirus infections are scarce. A study performed with patients infected by the hantavirus *Puumala virus* – which causes HFRS – showed hilar and mediastinal lymphadenopathy in only a minority of cases [57]. The authors suggested that lymphadenopathy was related to capillary leakage and overall fluid overload, as these patients also presented with pleural effusion and pericardial fluid. In addition, Rovida et al. [58] reported a case of HPS presenting diffuse nodular infiltrates associated with lymphadenopathy.

Thoracic lymph node abnormalities are not commonly found in immunocompetent patients with influenza virus infections. Verrastro et al. [59] described the spectrum of CT findings in nine patients with laboratory-confirmed influenza A infection. Mediastinal lymphadenopathy was found in two of the subjects. In a similar study, lymphadenopathy was found in two of three subjects. The nodes enhanced homogeneously, measured 1 cm along the short axis, and involved the right hilar, carinal, and subcarinal nodal stations [60].

The clinical spectrum of dengue virus infection ranges from asymptomatic to severe illness [61]. Physical examination often reveals generalized lymphadenopathy, as –following a bite by an infected mosquito– the virus replicates in the regional lymph nodes and is disseminated via the lymph and blood to other tissues [62–64].

Although most viral infections in immunocompetent persons are self-limited, some patients can develop pneumonia (when parenchymal involvement occurs). In such cases, follow-up chest imaging after diagnosis is important to ensure that a pulmonary malignancy is not missed [65].

1.10. Heart failure

Chronic left heart failure may cause mediastinal lymphadenopathy. Several mediastinal lymphatic chains are involved, but the subcarinal, paratracheal, and hilar nodes are more frequently affected. The mechanisms underlying the pathogenesis of lymphadenopathy in cardiogenic pulmonary edema are not completely clear, but it has been suggested to be the expression of diffuse

intrathoracic edema affecting the pulmonary parenchyma and neighboring structures, including the mediastinum and associated lymph nodes [66]. Lymphadenopathy has been suspected based on features observed on radiographs taken to investigate dyspnea and heart failure. The identification of suspicious features is theoretically easier on follow-up radiographic examinations, which provide better visibility of hilar and mediastinal areas, after treatment to reduce pulmonary edema [66].

1.11. Idiopathic pulmonary fibrosis

Idiopathic pulmonary fibrosis (IPF) is a specific form of chronic fibrosing interstitial pneumonia limited to the lung [67]. The reported prevalence of mediastinal lymphadenopathy in IPF is 66% (90/136 patients) [68] or, similarly, 70% [69]. The presence of enlarged mediastinal nodes may indicate a more chronic and advanced disease process [70]. Jung et al. [71] showed that the total number of enlarged lymph nodes increased with the severity score of pulmonary fibrosis.

IPF was reported to be associated with an increased risk of lung cancer, due to the occurrence of atypical or dysplastic epithelial changes in fibrosis, which progress to invasive malignancy [72]. Consensus on this association is lacking, but epidemiological reports have described an increased incidence of lung cancer during IPF follow-up. In addition, lung cancer was found simultaneously with IPF in some autopsy studies [73]. The relation between the IPF severity score of – reflected in the number of enlarged lymph nodes – and the emergence of lung cancer also remains uncertain and offers a potential area for further investigation [67,72].

1.12. Chronic obstructive pulmonary disease

COPD is characterized by progressive airflow obstruction, inflammation in the airways, and systemic effects or comorbidities [74]. Approximately 50% of patients with COPD present enlarged hilar and mediastinal lymph nodes. These lymph nodes are located predominantly in the lower paratracheal space, in the aortopulmonary window, and below the carina. Lymph node enlargement is identified more often in patients with signs of severe bronchitis, which seems to be logical because the inflammatory processes seen in chronic bronchitis may result in airway remodeling and narrowing and reactive nodal enlargement. All enlarged lymph nodes in patients with COPD have well-defined contours, and most are oval. Neither calcification nor central low attenuation of enlarged lymph nodes is seen in the majority of patients [75].

1.13. Pulmonary embolism

Lymphadenopathy is common in patients with pulmonary arterial hypertension caused by proven chronic pulmonary thromboembolism, and may not necessarily implicate additional pulmonary disease. Enlarged nodes are found on CT in more than one-third of patients with chronic pulmonary thromboembolism with no clinical or radiological evidence of comorbid conditions. The frequent association between enlarged hilar lymph nodes and pleural and pericardial effusions raises the possibility of a common pathophysiological mechanism related to the slowing of lymphatic flow in the mediastinum, caused by increased pressure in the systemic venous system [76].

1.14. Drug-induced lymphadenopathy

Hypersensitivity reactions to drugs can cause mediastinal or hilar lymph node enlargement. Anticonvulsants, particularly phenytoin, can cause a pseudolymphoma syndrome with generalized lymphadenopathy in addition to fever, skin rash, eosinophilia, and hepatosplenomegaly. Methotrexate, sulfonamides, penicillin, allopurinol, aspirin, and erythromycin are other examples of drugs with this effect. These reactions tend to follow several months of drug therapy and decrease after discontinuation of the drug [7].

Table 1
Main features of benign lymphadenopathy.

High density	Asymmetrical	Bilateral	Calcification
Sarcoidosis		x	x
Silicosis		x	x
Amyloidosis		x	x
Berylliosis		x	x
Tuberculosis	x		x
Castleman's disease	x		
Normal Density			
Heart failure			
Pulmonary fibrosis			
COPD			
Drug-induced lymphadenopathy	x		
Pulmonary embolism			
Viral infection		x	
Low Density			
Tuberculosis	x		x
Fungal infection	x		x

The main characteristics of the previously described lymphadenopathies are summarized in Table 1.

2. Conclusion

Patterns of thoracic lymphadenopathy can provide important clues to the diagnosis of many benign diseases. Careful evaluation of these findings is important to decrease the number of unnecessary interventions. Knowledge of the limitations of size and site criteria in predicting nodal status is important to correctly indicate the need for follow-up imaging or pathological confirmation.

References

[1] R. Ferrer, Lymphadenopathy: differential diagnosis and evaluation, Am. Fam. Physician 58 (1998) 1313–1320.
[2] G. Macis, A. Cina, A. Pedicelli, G. Restaino, F. Molinari, Lymph node imaging: from conventional radiology to diagnostic imaging, Rays 25 (2000) 399–417.
[3] T. Suwatanapongched, D.S. Gierada, CT of thoracic lymph nodes. Part II: diseases and pitfalls, Br. J. Radiol. 79 (2006) 999–1000.
[4] H. Bayanati, E. Tornhill, C.A. Souza, V. Sethi-Virmani, A. Gupta, D. Maziak, et al., Quantitative CT texture and shape analysis: can it differentiate benign and malignant mediastinal lymph nodes in patients with primary lung cancer? Eur. Radiol. 25 (2015) 480–487.
[5] S. Ganeshalingam, D.M. Koh, Nodal staging, Cancer Imaging 9 (2009) 104–111.
[6] J. Burrill, C.J. Williams, G. Bain, G. Conder, A.L. Hine, R.R. Misra, Tuberculosis: a radiologic review, Radiographics 27 (2007) 1255–1257.
[7] J.R. Brown, A.T. Skarin, Clinical mimics of lymphoma, Oncologist 9 (2004) 406–416.
[8] L.H. Schwartza, J. Bogaertsb, R. Fordc, L. Shankard, P. Therassee, S. Gwytherf, et al., Evaluation of lymph nodes with RECIST 1.1, Eur. J. Cancer 45 (2009) 261–267.
[9] K. Kiyono, S. Sone, F. Sakai, Y. Imai, T. Watanabe, I. Izuno, et al., The number and size of normal mediastinal lymph nodes: a postmortem study, AJR Am. J. Roentgenol. 150 (1988) 771–776.
[10] T. Suwatanapongched, D.S. Gierada, CT of thoracic lymph nodes. Part I: anatomy and drainage, Br. J. Radiol. 70 (2006) 922–928.
[11] P.A. De Jong, R.J. Nievelstein, Normal mediastinal and hilar lymph nodes in children on multi-detector row chest computed tomography, Eur. Radiol. 22 (2012) 318–321.
[12] A.N. Leung, Pulmonary tuberculosis: the essentials, Radiology 210 (1999) 307–322.
[13] R.P. Maheshwarappa, A. Gupta, J. Bansal, M.L. Meena, Spectrum of tuberculosis in human body – a radiologic review, IOSR–JDMS 10 (2013) 36–54.
[14] Y.J. Jeong, K.S. Lee, Pulmonary tuberculosis: up-to-date imaging and management, AJR Am. J. Roentgenol. 191 (2008) 834–844.
[15] R. Kurowski, M. Ostapchuk, Overview of histoplasmosis, Am. Fam. Physician

66 (2002) 2247–2252.
[16] S.E. Rossi, H.P. McAdams, M. Rosado-de-Christenson, T.J. Franks, J.R. Galvin, Fibrosing mediastinitis, Radiographics 1 (2001) 737–757.
[17] J.E. Loyd, B.F. Tillman, J.B. Atkinson, R.M. des Prez, Mediastinal fibrosis complicating histoplasmosis, Med. Baltim. 67 (1988) 295–310.
[18] C.M. Jude, M.B. Nayak, M.K. Patel, M. Deshmukh, P. Batra, Pulmonary coccidioidomycosis: pictorial review of chest radiographic and CT findings, Radiographics 34 (2014) 912–925.
[19] D. Capone, E. Marchiori, B. Wanke, K.E. Dantas, M.A. Cavalcanti, A. Deus-Filho, et al., Acute pulmonary coccidioidomycosis: CT findings from 15 patients, Br. J. Radiol. 81 (2008) 721–724.
[20] N.F. Crum, E.R. Lederman, C.M. Stafford, J.S. Parrish, M.R. Wallace, Coccidioidomycosis: a descriptive survey of a reemerging disease—clinical characteristics and current controversies, Medicine 83 (Baltimore) (2004) 149–175.
[21] G.R. Thompson, Pulmonary coccidioidomycosis, Semin. Respir. Crit. Care. Med. 32 (2011) 754–763.
[22] A.P. Mayer, M.F. Morris, P.M. Panse, M.G. Ko, J.A. Files, B.E. Ruddy, et al., Does the presence of mediastinal adenopathy confer a risk for disseminated infection in immunocompetent persons with pulmonary coccidioidomycosis? Mycoses 56 (2013) 145–149.
[23] The American Thoracic Society (ATS), The European Respiratory Society (ERS), The World Association of Sarcoidosis and Other Granulomatous Disorders (WASOG), Statement on sarcoidosis, Am. J. Respir. Crit. Care. Med. 160 (1999) 736–755.
[24] H. Al-Jahdali, P. Rajiah, S.S. Koteyar, C. Allen, A.N. Khan, Atypical radiological manifestations of thoracic sarcoidosis: a review and pictorial essay, Ann. Thorac. Med. 8 (2013) 186–196.
[25] B.H. Miller, M.L. Rosado-de-Christenson, H.P. McAdams, N.F. Fishback, Thoracic sarcoidosis: radiologic-pathologic correlation, RadioGraphics 15 (1995) 421–437.
[26] E.F. Conant, M.F. Glickstein, P. Mahar, W.T. Miller, Pulmonary sarcoidosis in the older patient: conventional radiographic features, Radiology 169 (1988) 315–319.
[27] E. Criado, M. Sánchez, J. Ramírez, P. Arguis, T.M. de Caralt, R.J. Perea, A. Xaubet, Pulmonary sarcoidosis: typical and atypical manifestations at high-resolution CT with pathologic correlation, Radiographics 30 (2010) 1567–1586.
[28] B. Satija, S. Kumar, U.C. Ojha, D. Gothi, Spectrum of high-resolution computed tomography imaging in occupational lung disease, Indian. J. Radiol. Imaging 23 (2013) 287–296.
[29] D.R. Baldwin, L. Lambert, C.F. Pantin, K. Prowse, R.B. Cole, Silicosis presenting as bilateral hilar lymphadenopathy, Thorax 51 (1996) 1165–1167.
[30] V.C.S. Antao, G.A. Pinheiro, M. Terra-Filho, J. Kavakama, N. Müller, High-resolution CT in silicosis: correlation with radiographic findings and functional impairment, J. Comput. Assist. Tomogr. 29 (2005) 350–356.
[31] K. Brown, D.F. Mund, D.R. Aberle, P. Batra, D.A. Young, Intrathoracic calcifications: radiographics features and differential diagnosis, Radiographics 14 (1994) 1247–1261.
[32] A.S. Ferreira, V.B. Moreira, H.M. Ricardo, R. Coutinho, J.M. Gabetto, E. Marchiori, Progressive massive fibrosis in silica-exposed workers, high-resolution computed tomography findings, J. Bras. Pneumol. 32 (2006) 523–528.
[33] C.G.C. Ooi, P.L. Khong, R.S.Y. Cheng, B. Tam, F. Tsang, I. Lee, et al., The relationship between mediastinal lymph node attenuation with parenchymal lung parameters in silicosis, Int. J. Tuberc. Lung. Dis. 7 (2003) 1199–1206.
[34] J. Murray, I. Webster, G. Reid, D. Kielkowski, The relation between fibrosis of hilar lymph glands and the development of parenchymal silicosis, Br. J. Ind. Med. 48 (1991) 267–269.
[35] A. Seaton, J.W. Cherrie, Quartz exposures and severe silicosis: a role for the hilar nodes, Occup. Environ. Med. 55 (1998) 383–386.
[36] J.M. Cox-Ganser, C.M. Burchfiel, D. Fekedulegn, M.E. Andrew, B.S. Ducatman, Silicosis in lymph nodes: the canary in the miner? J. Occup. Environ. Med. 51 (2009) 164–169.
[37] C.S. Georgiades, E.G. Neyman, M.A. Barish, Amyloidosis: review and CT manifestations, Radiographics 24 (2004) 405–416.
[38] E.M. Capitani, A.M.A. Altemani, J.I. Kawakama, Pulmonary beriliosis: literature review and case report, J. Pneumol. 21 (1995) 135–142.
[39] C.W. Cox, C.S. Rose, D.A. Lynch, State of the Art: Imaging of Occupational Lung Disease, Radiology 270 (2014) 681–696.
[40] T. Dégot, A. Métivier, S. Casnedi, M. Chenard, R. Kessler, Thoracic manifestations of Castleman's disease, Rev. Pneumol. Clin. 65 (2009) 101–107.
[41] H.P. McAdams, M. Rosado-de-Christenson, N.F. Fishback, P.A. Templeton, Castleman disease of the thorax: radiologic features with clinical and histopathologic correlation, Radiology 209 (1998) 221–228.
[42] H. Racil, S. Cheikh Rouhou, O. Ismail, S. Hantous-Zannad, N. Chaouch, M. Zarrouk, et al., Castleman's disease: an intrapulmonary form with intrafissural development, Sci. World J. 14 (2009) 940–945.
[43] P. Agrawal, S. Naseem, N. Varma, P. Sharma, P. Malhorta, S. Varma, Bone marrow involvement in multicentric castleman disease in a HIV negative patient, Indian J. Hematol. Blood Transfus. 30 (2014) 940–945.
[44] S.H. Zhu, Y.H. Yu, Y. Zhang, J.J. Sun, D.L. Han, J. Li, Clinical features and outcome of patients with HIV-negative multicentric Castleman's disease treated with combination chemotherapy: a report on 10 patients, Med. Oncol. 30 (2013) 492.
[45] M.E. Gatti-Mays, D. Kardon, T.T. Chieu, K. Firozvi, Autoimmune pancreatitis in the setting of multifocal Castleman disease in an HIV-negative, HHV-8-negative, 70-year-old man, Clin. Adv. Hematol. Oncol. 10 (2012) 683–686.
[46] R. Barker, F. Kazmi, M. Bower, Imaging in multicentric Castleman's disease, J. HIV Ther. 13 (2008) 72–74.
[47] A. Guihot, L.J. Couderc, E. Rivaud, L. Galicier, P. Bossi, E. Oksenhendler, et al., Thoracic radiographic and CT findings of multicentric Castleman disease in HIV-infected patients, J. Thorac. Imaging 22 (2007) 207–211, 41.
[48] E.A. Kim, K.S. Lee, S.L. Primack, H.K. Yoon, H.S. Byun, T. Kim, et al., Viral pneumonias in adults: radiologic and pathologic findings, Radiographics 22 (2002) 137–149.
[49] T. Franquet, Imaging of pulmonary viral pneumonia, Radiology 260 (2011) 18–39.
[50] J.S. Friedland, G. Santis, M.J. Smith, Infectious mononucleosis: a cause of bilateral hilar lymphadenopathy, Postgrad. Med. J. 64 (1988) 799–800.
[51] C.A. Gogos, H.P. Bassaris, A.G. Vagenakis, Varicella pneumonitis in adults: a review of pulmonary manifestations, risk factors and treatment, Respiration 59 (1992) 339–343.
[52] A.H. Mohsen, M. McKendrick, Varicella pneumonia in adults, Eur. Respir. J. 21 (2003) 886–891.
[53] J.S. Kim, C.W. Ryu, S.I. Lee, D.W. Sung, C.K. Park, High-resolution CT findings of varicella-zoster pneumonia, AJR Am. J. Roentgenol. 72 (1999) 113–116.
[54] T.M. Maher, N.K. Gupta, M.M. Burke, M.R. Carby, CT findings of varicella pneumonia after lung transplantation, AJR Am. J. Roentgenol. 188 (2007) W557–W559.
[55] E.N. Sargent, M.J. Carson, E.D. Reilly, Roentgenographic manifestations of varicella pneumonia with postmortem correlation, Am. J. Roentgenol. Radium Ther. Nucl. Med. 98 (1966) 305–317.
[56] C.J. Peters, G.L. Simpson, H. Levy, Spectrum of hantavirus infection: hemorrhagic fever with renal syndrome and hantavirus pulmonary syndrome, Annu. Rev. Med. 50 (1999) 531–545.
[57] A. Paakkala, R. Järvenpää, S. Mäkelä, H. Huhtala, J. Mustonen, Pulmonary high-resolution computed tomography findings in nephropathia epidemica, Eur. J. Radiol. 81 (2012) 1707–1711.
[58] F. Rovida, E. Percivalle, A. Sarasini, G. Chichino, F. Baldanti, Imported hantavirus cardiopulmonary syndrome in an Italian traveller returning from Cuba, New Microbiol. 36 (2013) 103–105.
[59] C.G.Y. Verrastrol, L. Abreu-Junior, D.Z. Hitomil, E.P. Antoniol, R.A. Neves, G. D'Ippolito, Manifestations of infection by the novel influenza A (H1N1) virus at chest computed tomography, Radiol. Bras. 42 (2009) 343–348.
[60] N.R. Qureshi, T.T. Hien, J. Farrar, F.V. Gleeson, The radiologic manifestations of H5N1 avian influenza, J. Thorac. Imaging 21 (2006) 259–264.
[61] G.H. Fijten, G.H. Blijham, Unexplained lymphadenopathy in family practice. An evaluation of theprobability of malignant causes and the effectiveness of physician's workup, J. Fam. Pract. 27 (1988) 373–376.
[62] A. Goel, D.N. Patel, K.K. Lakhani, S.B. Agarwal, A. Agarwal, S. Singla, et al., Dengue fever – a dangerous foe, JIACM 5 (2004) 247–258.
[63] S. Rao, A. Loya, K.S. Ratnakar, V.R. Srinivasan, Lymph node infarction – a rare complication associated with disseminated intra vascular coagulation in a case of dengue fever, BMC Clin. Pathol. 5 (2005) 1–5.
[64] V. Lo Re, S.J. Gluckman, Fever in the returned traveler, Am. Fam. Physician 68 (2003) 1343–1350.
[65] E.M. Mortensen, L.A. Copeland, M.J. Pugh, Diagnosis of pulmonary malignancy after hospitalization for pneumonia, Am. J. Med. 123 (2010) 66–71.
[66] A. Ngom, P. Dumont, P. Diot, E. Lemarié, Benign mediastinal lymphadenopathy in congestive heart failure, Chest 119 (2001) 653–656.
[67] J. Park, D.S. Kim, T.S. Shim, C.M. Lim, Y. Koh, S.D. Lee, et al., Lung cancer in patients with idiopathic pulmonary fibrosis, Eur. Respir. J. 17 (2001) 1216–1219.
[68] C.A. Souza, N.L. Muller, K.S. Lee, T. Johkoh, H. Mitsuhiro, S. Chong, Idiopathic interstitial pneumonias: prevalence of mediastinal lymph node enlargement in 206 patients, AJR Am. J. Roentgenol. 168 (2006) 995–999.
[69] H. Niimi, E.Y. Kang, J.S. Kwong, S. Carignan, N.L. Müller, CT of chronic infiltrative lung disease: prevalence of mediastinal lymphadenopathy, J. Comput. Assist. Tomogr. 20 (1996) 305–308.
[70] M.K. Lim, J.G. Im, J.M. Ahn, J.H. Kim, S.K. Lee, K.M. Yeon, et al., Idiopathic pulmonary fibrosis vs. pulmonary involvement of collagen vascular disease: HRCT findings, J. Korean Med. Sci. 12 (1997) 492–498.
[71] J.I. Jung, H.H. Kim, Y.J. Jung, S.H. Park, J.M. Lee, S.T. Hahn, Mediastinal lymphadenopathy in pulmonary fibrosis: correlation with disease severity, J. Comput. Assist. Tomogr. 24 (2000) 706–710.
[72] R. Haddad, D. Massaro, Idiopathic diffuse interstitial pulmonary fibrosis (fibrosing alveolitis), a typical epithelial proliferation and lung cancer, Am. J. Med. 45 (1968) 211–219.
[73] A. Nagai, A. Chiyotani, T. Nakadate, K. Konno, Lung Cancer in Patients with idiopathic pulmonary fibrosis, Tohoku J. Exp. Med. 167 (1992) 231–237.
[74] M. Decramer, W. Janssens, M. Miravitlles, Chronic obstructive pulmonary disease, Lancet 379 (2012) 1341–1351.
[75] J. Kirchner, E.M. Kirchner, J.P. Goltz, A. Obermann, R. Kickuth, Enlarged hilar and mediastinal lymph nodes in chronic obstructive pulmonary disease, J. Med. Imaging Radiat. Oncol. 54 (2010) 333–338.
[76] C.J. Bergin, K.J. Park, Lymph node enlargement in pulmonary arterial hypertension due to chronic thromboembolism, J. Med. Imaging Radiat. Oncol. 52 (2008) 18–23.